Smart Materials and Structures, Volume 23, Number 3, 035010

Strong electron emissions induced and extracted by pyroelectric crystals

M. Hockley and Z. Huang

Manufacturing and Materials Department, School of Applied Sciences,

Cranfield University, Bedfordshire, MK43 0AL, UK

Abstract

A high voltage pulse generated by changing the temperature of a pyroelectric crystal was used to induce strong electron emissions from a ferroelectric cathode. The effects of the extracting voltage provided by an external power source or by another pyroelectric crystal on the electron emission property were investigated. Similar as for normal ferroelectric cathode, both the electron emission current and the total emitted electrons were found to increase with the increasing extracting voltage. However, the final voltage on the cathode after electron emission was also found to depend on the extracting voltage at the anode. The electron emission was also found to depend not only on the pulse generation and the ferroelectric cathode as reported previously, but also on the capacitance of the anode. These phenomena were explained by surface-plasma-assisted electron emission mechanism.

1. INTRODUCTION

There has been extensive research in the past several years on portable and compact devices for electron, ion, and X-ray generation using pyroelectric crystals. Pyroelectric crystals exhibit a change in polarization (P) proportional to the crystal's pyroelectric coefficient (p) times the magnitude of the temperature change (ΔT) when heated or cooled, $P=p \bullet \Delta T$ [1]. These polarization charges are usually compensated by screening charges in atmospheric conditions. In a vacuum, however, the complete screening may take a very long time [2], so there is a built up of net charges on the crystal surface when there is a rapid change of temperature in the crystal. These non-compensated charges were able to produce an electric field strong enough to eject electrons from the crystal surface and then accelerate them to high velocity [3], which in turn, can ionise more gas molecules to produce more electrons and ions. When these high energy electrons strike a metal target or a pyroelectric crystal, both the characteristic X-rays of the target and the X-ray continuum of bremsstrahlung associated with the deceleration of the electrons striking the target are produced [4-6]. Electron beams [7,8], ion beams [9], even neutrons [10,11] have been produced based on the same principle. As the electrons and ions are produced by the ionization of gas molecules, the intensity and the energy of the produced radiation are inter-related, there is usually an optimum gas pressure for a particular application. If the pressure is too high, it is impossible to build up a high enough electric field at the surface of the pyroelectric crystal, so only the low energy X–rays could be generated. On the other hand, if the pressure is too low, the mean free path of the electron will be too long and there will be little induced gas molecular ionization by fast electrons, which leads to weak intensity [12].

The above mentioned electron emission is called "weak" ferroelectric electron emission (FEE), as its current density is usually 10^{-12}-10^{-9} A/cm^2. For high intensity electron emission there is another technique called strong ferroelectric electron emission [13,14]. Strictly speaking it should not be called strong FEE because it does not depend on the ferroelectric switching as was initially

believed, indeed it can be generated in different phases of ferroelectric ceramics such as the ferroelectric, antiferroelectric, relaxor and even paraelectric states. It can be 10-12 orders of magnitude higher than the "weak" FEE, and can achieve sometimes current density of more than 100 A/cm^2 [14]. Strong FEE is usually excited using a patterned electrode (strip, grid, or ring) deposited on the polar ferroelectric surface and triggered by a voltage pulse range from a few hundred to tens of thousand of volts. The emitted electrons have low energy <400 eV when there is no extracting voltage [14,15]. Usually an extracting voltage is applied to accelerate the electrons to high velocity [14,16]. Ferroelectric cathode based on this mechanism was able to supply one order of magnitude higher current as compared to the thermionic one under the same conditions [17].

The strong FEE is generally believed to be a plasma-assisted electron emission [14-19]. The emission mechanism is the same as for the metal-dielectric cathodes, which have been in use for many years. When a driving voltage pulse is applied to the rear (or front) electrode of the ferroelectric material, a tangential component as well as the normal component of the applied electron field is created [20]. In the triple points where metal, vacuum, and the ferroelectric material meet the electric field is increased by a factor of ε_r. Here ε_r is the relative dielectric constant of the dielectric material [21], as a result field electron emission occurs at the triple junctions [22]. The emitted electrons then multiply as an avalanche traversing the dielectric surface due to the tangential component of the electric field, which leads to the formation of the surface plasma, and this surface plasma provides electrons for the strong FEE [14, 23]. It is claimed that this surface plasma can serve as an almost unlimited source of electrons for a strong electron beam current [14]. For strong FEE or metal-dielectric cathodes, usually a bulky high voltage pulse generator is needed as a power source.

We have reported a novel method of producing strong electron emission by combining strong FEE with pyroelectric crystals. No external pulse generator was needed. Instead, a high voltage was

generated by changing the temperature of a pyroelectric crystal, and in conjunction with a miniature spark gap switching device, a high voltage pulse was generated and then used to trigger strong FEE [24, 25]. It has been concluded that when a negative pulse was applied to the front electrode of the cathode, the electron emission current and total charges were the greatest when there was no extracting voltage [24, 25].

In this communication, we report the investigation of the effect of an extracting voltage on the electron emission properties of the pyroelectric induced electron emission system. Firstly an external extracting voltage was used. Through the monitoring of the pulse, cathode, and anode components, the mechanisms behind the observed features were investigated and methods to improve the electron emission property of the device were proposed. And finally the electron emission properties when the extracting voltage was supplied by another pyroelectric crystal were investigated.

2. EXPERIMENTAL

2.1.Pyroelectric crystal induced and extracted electron emission

A schematic of the pyroelectric crystal induced and extracted set-up for electron emission is shown in figure 1(a). Its equivalent circuit is shown in figure 1(b). Briefly, a pyroelectric crystal $LiTaO_3$ (b, C_{py1}, LT) of dimensions 10x5x5 mm^3 was attached to a Peltier temperature controller (a, Supercool PR-59). The polarization vector was in the 10 mm direction and its Z^+ surface is connected to a miniature spark gap (g, Littlefuse CG3), so that heating the crystal b will produce a negative voltage on the Z^+ surface. The LT crystal was electroded with conductive epoxy and was connected in parallel to a charging capacitor C_{chg} to increase the capacitance of the charging system, then they are connected to a miniature spark gap g, before connected to the front electrode e of the

ferroelectric cathode. The back electrode d was connected to the ground. The ferroelectric cathode consisted of an unpoled lead zirconate titanate (PZT) ceramic (PZ34, Ferroperm Piezoceramic A/S) with a relative dielectric constant ε_r=210 and dimensions of 10x10x0.4 mm^3, fully metallised back electrode, and patterned front electrode made of copper grids of 3.05 mm diameter, which is usually used as a sample holder for transmission electron microscope. The copper grid was connected to the PZT, and then electric wires were epoxy connected to both the front and rear electrodes. The voltage on the cathode was monitored by an oscilloscope (MSO6104A, Agilent Technologies) using a voltage divider consisted of two resistors of 100 MΩ and 1 MΩ. The high resistance (101 MΩ) of this divider combined with the cathode capacitance of about 30 pF gives a time constant of about 3 ms for the cathode system. This is compared to the typical duration of an emission event of about 2 μs. This ensured minimal loading by the measurement system during the electron emission.

Another pyroelectric crystal LT (K, C_{py2}) was connected to the anode f , and a voltage/charge measurement system was constructed. The LT crystal K was orientated such that heating it would produce a positive voltage on its top surface (Z^-). Inside the vacuum chamber a Peltier element sitting on an aluminium plate was used to control the temperature of this LT. A heat sink was bonded to the other side of the plate which sit outside of the vacuum chamber. This maintained one side of the Peltier at close to room temperature. The aluminium plate, and therefore the bottom side of the LT was electrically grounded. A thermistor was used for temperature monitoring, via the Supercool PR-59 temperature controller. A temperature ramp rate of 20°C per minute was used for heating the LT crystals.

To determine the voltage on the anode f a voltage follower circuit (op 741) was used in conjunction with a capacitive voltage divider, which consisted of C_{acc} and C_2 in series connection (Figure 1(b). Notice in figure 1(a) some components for measurement were omitted for clarity reason. The C_{acc} capacitor of the divider also served the purpose of charge storage capacitor for the LT crystal K.

For this work, we had C_{acc}=10 or 50 pF, C_2= 68 nF, so the voltage output to the oscilloscope was always very small and within the allowed range.

To measure the charge collected by the anode, the anode was connected coaxially to a 50Ω resistor. Through which the voltage was monitored by an oscilloscope (MSO6104A, Agilent Technologies) via a probe directly. The voltage follower op 741 could not be used since it does not have the sufficient slew rate, which led to significant signal distortion.

2.2.External voltage extracted electron emission

For external voltage extracted electron emission, most of the set-up were the same as above. The differences were an external HV source (GBS Elektronik GmbH, RUP3-25a) was connected to the anode f, to replace the Anode subsystem in figure 1(b) ; and a measurement system was connected for the pulse generating crystal b (C_{py1}) rather than for the crystal K (C_{py2}). The equivalent circuit is shown in figure 1(c). For safety consideration, the extracting voltage was never allowed to be higher than 6 kV, in order to avoid the production of hazardous X-rays. The cathode was always fired in the 'negative pulse to front electrode' regime for these experiments, since this produce the greatest electron emissions [24]. The DC voltage was applied prior to an emission event. The voltage on the LT crystal b was monitored using a voltage follower circuit (OP 741) connected to the output of a capacitive voltage divider C_{chg} and C_2. This voltage follower had a very high input impedance of at least 1.5 TΩ, in order to prevent charge leakage in the measurement system. The C_{chg} capacitor of the divider also served the purpose of charge storage capacitor for the LT C_{py1}. For this work, we had C_{chg}=22 pF, C_2= 68 nF, so the voltage output to the oscilloscope was always small and within the allowed range.

In all the experiments a 12.5 mm diameter anode f was used and was placed 10 mm from the cathode. All experiments were conducted under a vacuum of approximately $2x10^{-5}$ Torr.

3. RESULTS AND DISCUSSIONS

3.1. External voltage extracted electron emission

Figure 2 depicts the voltage on the cathode, the current and total charges collected at the anode as functions of time, when a 50 mesh ϕ3.05 mm copper grids was used as the front electrode of the cathode and the external extracting voltage at the anode was (a) 227 V, and (b) 1610 V, respectively. The spark gap switch on time was taken as time zero. When the extracting voltage was low at 227 V, the cathode voltage reached -2340 V at about 40 ns, then gradually increased to -250 V at about 860 ns, and then slightly decreased again to around -340 V at about 1 μs and stabilised around that value thereafter. The electron emission was collected from about 120 ns, peaked at about 39 mA (current density 31 mA/cm^2) at 760 ns, then gradually decreased to nothing at about 2 μs. When the extracting voltage was increased, the peak current and the total collected charge also increased, although the emission duration was remained around 2 μs. However, the final stabilised voltage on the cathode electrode after the electron emission increased with the increasing extracting voltage (Figure 3). This indicates that whilst the electrons in the surface plasma were emitted to the anode, the positively charged ions were repelled to the grid electrode, and the voltage on the grid electrode could be higher than the voltage on the anode.

To shed light on the emission process the voltage evolution with time for the pyroelectric charging components C_{chg} was also investigated. Figure 4 shows time profiles for the voltage V_{cat} on the cathode front electrode, the voltage V_{chg} on the charging capacitor C_{chg}, and the collected current I_{anode} at the anode, for different extracting voltages, (a) 0 V; (b) 200 V; and (c) 600 V. Again, it can be observed that the final stabilised voltage on the cathode increased with the increasing extracting voltage, the same as discussed above. Furthermore, the final stabilised voltage V_{chg} on the

pyroelectric crystal b (C_{py1}) and the charging capacitor C_{chg} was also found to vary with the extracting voltage, as shown in figure 5. This suggests an increasing charge transfer from the pulse subsection to the cathode subsection with the increasing extracting voltage. Also, V_{chg} and V_{cat} were approximately the same when the extracting voltages were between 100 to 300 V (Figure 4b). This suggests that the spark gap was kept on for some time after the emission started. When electrons were emitted to the anode, the positively charged ions from the surface plasma were emitted to the grid electrode of the cathode, which lead to the increase of the potential on the grid electrode. Charge transfer between the charging capacitor C_{chg} and the cathode grid electrode will take place if the spark gap was "on". The above results suggest an effect of the extracting voltage on the surface plasma development of the cathode. However, the exact mechanism behind it remains unclear. Nevertheless, this implies that it may be possible to make the charging components (the pyroelectric crystal b and the charging capacitor C_{chg}) electrically neutral after each pulse generation through the careful choice of the operational parameters and the specifications of the spark gap switching device.

The positive voltage on the cathode is detrimental to the electron emission, it should be avoided. One solution was to connect a diode (FHV03-12, FCI Semiconductor) between the grid electrode and the ground, as shown in figure 6. When V_{cat} is negative, this diode is at "off" state, no current can flow through. However, when V_{cat} is positive and greater than a certain value, the diode is "on", and electrons from the ground will be able to flow through the diode and cancel out or reduce the positive potential on the cathode, which in turn should help the electron emission to the anode. Table 1 summarises measurement results for the electron emissions induced by a pyroelectric crystal and extracted by an external voltage, when a diode was (or was not) connected between the cathode and ground. A negative pulse was applied to the front electrode of the cathode, the nominal break down voltage for the spark gap was 1.5 kV. The extraction voltage, peak current, and total charges were all measured at the anode. The pyro charges were obtained using the measured

pyroelectric coefficient p=1.46 x10^{-4} C cm^{-2} K^{-1}. The ratio of the total collected charges to the total charges produced by the pyroelectric crystal during the temperature change is listed in the last column. From this table and figure 7 it can be seen that the emission current and total collected charges increased with the increasing extracting voltage, and the total emitted charges can be greater than the charges generated by the pyroelectric crystal b due to its temperature change. Figure 7 and Table 1 also show that with the addition of a diode, the emitted charges and the emission current were increased under the same extracting voltage when the extracting voltage was higher than a certain value (500 V). However, the final voltages on the cathode did not reduce to zero even with a diode connected, this was probably due to the limited current through the diode in the short time period. A diode with a high allowable current and shorter response time is expected to increase the discharging current and improves the electron emission further.

3.2.Pyroelectric crystal induced and extracted electron emission

The pyroelectric voltages as functions of the temperature change of the pyroelectric crystal LT when the C_{acc} were 10 pF and 50 pF were measured by experiments at first. The linear relationships between the generated voltage and the temperature change were confirmed. Assuming the LT crystal had a pyroelectric coefficient p, and the circuit had a stray capacitance C_{stray}. We have $V = p \bullet A \bullet \Delta T/(C_{acc} + C_{stray} + C_{py2})$, here A=25 x 10^{-6} m^2 was the area of the pyro crystal surface, C_{py2}= 1.02 pF was the capacitance of the LT crystal assuming its relative dielectric constant being 46. We therefore obtained p = 1.46 x10^{-4} C $m^{-2}K^{-1}$, and C_{stray}= 2.2 pF. This value of pyroelectric coefficient was smaller than the usually reported value for this crystal, but it should not affect the accurancy of the calculated pyroelectric charges for a particular temperature change in this work.

The strong ferroelectric electron emission (FEE) triggered by a pyroelectric crystal and extracted by a pyroelectric anode was then investigated. Two acceleration capacitances C_{acc} =10 pF and 50 pF

were used. Experiments with each of these values were conducted with and without a shunt diode being connected between the front electrode of the cathode and the ground, resulting in a total of four configurations. Table 2 shows that the collected charge ranged from -3.0 nC at V_{acc} = 0 V to -41.3 nC at V_{acc} = 5063 V with C_{acc} = 10 pF and with a shunt diode connected. All result showed a general increase in the amount of collected charge with the increasing V_{acc}. The specifics of each case differed however and will be discussed below.

Figure 8 depicts the total collected emission charges as functions of the extracting voltage generated by a pyroelectric crystal with or without a shunt diode being connected when the C_{acc} were (a) 50, and (b) 10 pF, respectively. This clearly shows that the collected charge was greater when the shunt diode was used for all but the lowest few values when C_{acc} was 50 pF. Also of note is the roughly linear trend of the data when the shunt diode was used, while without the shunt diode the trend levels off as V_{acc} was higher than 2 kV. However, in the case of C_{acc} = 10 pF, there appears to be no apparent difference between the data with and without the diode, with both cases showing nearly identical values for collected charge across the entire range of V_{acc}, as well as both showing a linear trend to the extracting voltage. A comparison of the collected charges of the emissions with a shunt diode connected when using C_{acc} = 10 pF, 50 pF, and an external voltage source with C_{acc} = 13 nF, is shown in Fig. 9. The results for without a shunt diode were similar. This shows that the external acceleration system gives the greatest total emission, with a greater difference with increasing V_{acc}.

The cathode voltage and emitted charges at the anode during the emission were monitored in order to shed light on the emission process. Figure 10 shows the time profiles for the (a) voltage on the cathode and (b) collected charges at the anode for different initial anode extracting voltages, when the C_{acc} was 50 pF and a shunt diode was connected between the cathode and ground. Every profile shows that the pulse initially dropped rapidly to a peak of a few thousand volts, then rose back, and

finally reached a stable value. Correspondently, the collected charges at the anode started to increase when the cathode voltage started to increase, and reached a plateau when the voltages at the cathode reached a stable value. The higher the anode extracting voltage, the longer it took for the cathode to reach a stable voltage and for the charges at the anode to reach a plateau. The time it took for the emission charge at the anode to reach a plateau were 290, 430 and 810 ns for the initial extracting voltages 0, 461, and 1189 V, respectively. Also, higher anode extracting voltage resulted in higher final electrical potential at the cathode and larger emission charges at the anode (Table 2). For these three extracting voltages, their respective final stabilised cathode voltages were -800, -430 and 130 V , and their respective collected emission charge were -3.2, -21.1, and -45.6 nC.

Compared to the cases when the charge collection anode was an plate connected to an external power source discussed earlier, or a Faraday Cup [24-25], the conclusion that the emission increased with the increasing extracting voltage was the same. However, there were some differences. When the collecting anode was a Faraday cup or an external voltage source, all the emissions lasted for about 2 μs. For the pyroelectric anode here, the emission lasted for less than 1 μs, and it became shorter for smaller extracting voltages (Figure 10). These can be explained by their different capacitance at the anode. For the pyroelectric accelerating systems, the anode had a small capacitance, so a small change of charges resulted a significant change of voltage (or potential) of the anode. The collection of the emitted electrons on the anode led to the reduction of the potential on the anode, and under certain conditions the potential at the anode could even became negative (for example when V_{acc} = 0 V, see Tables 2) which will repel electrons from the anode. Combining the fact that the potential on the cathode increased with emission and even became positive under some conditions (Figure 10(a)), further emission of electrons were stopped by these electric fields. Higher extracting voltage meant more positive charges were available at the anode, so longer emissions were allowed. It is this reduction of the extracting voltage on the anode during charge collection that caused the variation in performance for different anode set-ups. Larger capacitance of the anode

meant the reduction of the extracting voltage was smaller for the same amount of the collected charges, therefore greater electron emission was allowed.

The different results for the different configurations as shown in figure 8 can also be explained by considering which section (anode or cathode) has the limited available charges. In the case of C_{acc} = 50 pF with no diode connected, the charges available for emission were those from the surface plasma at the cathode. In the case of a 50 pF C_{acc} with a shunt diode connected, however, as long as there were positive voltages on the anode and surface plasma existed at the cathode, electrons can be emitted due to replenishment of the electrons through the diode. Therefore the limiting factor in this case was the supply of charges on the anode. Since the charge collected by the system with the diode connected is determined mostly by the charge on the anode C_{acc}, the amount of collected charge should be linear with V_{acc}. In the case of the two set-ups with C_{acc} = 10 pF, due to the small capacitance in C_{acc} relative to the C_{chg} (50 pF), either with or without a shunt diode being connected between the cathode and ground, the limiting source of charges was the anode. This means that the shunt diode should have little effect, since the charges present on the cathode were already more than that the anode can collect, therefore in both cases the collected charges increased linearly with V_{acc}.

When the capacitance of the anode became smaller, or the extracting voltages were higher, more complex behaviours were observed. Figure 11 shows time profiles of (a) the voltage on the cathode and (b) collected emission charges at the anode, when C_{acc} was 10 pF and no diode was connected between the cathode and ground. Again, as the extracting voltage was increased, the emission time became longer and the emitted charges were greater (Figure 11(b)). The collected charges were -2.7, -14.5, -30.9 and -40.9 nC for the initial anode voltages of 0, 1853, 3430 and 5008 V, respectively. However, the final stabilised voltage at the cathode firstly increased with the increasing anode voltage, (from -1337 to -1150 V when V_{acc} were changed from 0 to 1853 V), then it decreased

with the increasing anode voltage (from -1368 to -1743 V when V_{acc} were changed from 3430 to 5008 V). These features remained true when a shunt diode was connected between the cathode and ground. Noticed also the cathode voltage was reduced modestly during the whole emission process when the initial anode voltage was 5008 V, from the peak voltage of -2400 V at 20 ns to -1806 V at 2 μs. This difference of 594 V was much smaller than the other three, as shown in figure 11(a). We believe this was due to the effect of a high extracting voltage on the development of the surface plasma at the cathode. We have observed that at higher external extracting voltages, there was a much higher charge transfer from the pulse section to the cathode section when the spark gap was switched on. The above results suggest that this may also have happened when the pyroelectric acceleration voltage was higher than 3430 V. The exact mechanism however is still unclear. This may have significant implication in practice, as this paves the way for the optimization of the system by adjusting component properties so that a re-setting for the pulse and cathode sections are not needed for multiple pulses generation. When these high energy electrons strike a metal target (anode) or a pyroelectric crystal, both the characteristic X-rays of the target and the X-ray continuum of bremsstrahlung associated with the deceleration of the electrons striking the target are produced. Voltage higher than 6 kV has not been attempted in this work due to safety consideration. Once an X-ray shield is in place, much higher voltages, up to 100 kV for example, should be able to be produced for extracting electron emission. A portable, miniature X-ray generation device with high energy and high intensity radiations could be developed in the future.

4. CONCLUSIONS

This work has demonstrated that it is possible to generate high energy and high intensity electron beams by combining pyroelectric crystals with metal-dielectric cathode. However, the total amount of electron emission depends very much on the exact configuration of the set-up, especially on the extracting voltage and the capacitances of the components of the system. For the extracting voltage less than 6 kV investigated so far:

(1) It was found that with the increasing extracting voltage, both the electron emission current and the total emitted electrons were increased. Whilst negatively charged electrons were emitted to the anode, the positively charged ions in the surface plasma were repelled to the grid electrode of the front cathode, which led to the rapid increase of the cathode voltage. By connecting a shunt diode between the cathode and ground, these positive charges can be discharged to earth, which can improve the electron emission significantly.

(2) A linear relationship between the emission current and the extracting voltage was obtained when a shunt diode is connected to the front grid electrode of the cathode, when the charge limiting factor was the anode.

(3) For the electron emission triggered and extracted by two different pyroelectric crystals, the electron emission was affected significantly by the capacitance, and the extracting voltage of the anode. Higher accelerating voltage and larger capacitance of the anode resulted in greater electron emission. Connecting a diode between the cathode and ground was found to be beneficial only under certain conditions, when the cathode was the charge limiting section.

Acknowledgments

We thank UK EPSRC (EP/G013934/1) for financial support and Dr Karsten Hansen of Meggitt Ferroperm Piezoceramics A/S for providing the PZT ceramics used in this research.

References

[1] Nye J F 1979 *physical properties of crystals* (Oxford: Oxford University Press)

[2] Kalinin S, Johnson C, and Bonnell D 2002 *J. Appl. Phys.* **91** 3816

[3] Rosenblum B, Braunlich P, and Carrico J P 1974 *Appl. Phys. Lett*. **25** 17

[4] Brownridge J D 1992 *Nature* **358** 287

[5] Brownridge J D and Shafroth S M 2001 *Appl. Phys. Lett*. **79** 3364

[6] Geuther J A and Danon Y 2005 *J. Appl. Phys.* **97** 104916

[7] Brownridge J D and Shafroth S M 2005 *J. Electrostatics* **63** 249

[8] Bourim E, Kim D, Kin V, Moon C, and Yoo I 2004 *J. Electroceramics* **13** 293

[9] Neidholdt E and Beauchamp J 2007 *Anal. Chem.* **79** 3945

[10] Naranjo B, Gimzewski J K and Putterman S 2005 *Nature* **434** 1115

[11] Geuther J, Danon Y and Saglime F 2006 *Phys. Rev. Lett.* **96** 054803

[12] Brownridge J D and Raboy S 1999 *J. Appl. Phys.* **86** 640

[13] Gundel H, Riege H, Wilson E J, Handerek J, and Zioutas K 1989 *Ferroelectrics* **100** 1

[14] Rosenman G, Shur D, Krasik Ya E, and Dunaevsky A 2000 *J. Appl. Phys.* **88** 6109 and references therein.

[15] Dunaevsky A, Krasik Ya E, Felsteiner J, and Dorfman S 1999 *J. Appl. Phys.* **85** 8464

[16] Dunaevsky A, Krasik Ya E, Felsteiner J, and Dorfman S 1999 *J. Appl. Phys.* **85** 8474

[17] Jiang B, Kirkman G and Reinhardt N 1995 *Appl. Phys. Lett.* **66** 1196

[18] Dunaevsky A, Chirko K, Krasik Ya E, Felsteiner J, and Bershtam V 2001 *J. Appl. Phys.* **90** 4108

[19] Peleg O, Chirko K, Gurovich V, Felsteiner J, Krasik Ya E, and Bershtam V 2005 *J. Appl. Phys.* **97** 113307

[20] Rosenman G, Shur D, Garb K, Cohen R and Krasik Ya E 1997 *J. Appl. Phys.* **82** 772

[21] Kofoid J 1960 *AIEE Trans.* **6** 991

[22] Mesyats G A 1994 *Tech. Phys. Lett.* **20** 8

[23] Puchkarev V P and Mesyats G A 1995 *J. Appl. Phys.* **78** 5633

[24] Hockley M and Huang Z, 2012 *Appl. Phys. Lett.* **101** 222901.

[25] Hockley M and Huang Z, 2013 *J. Appl. Phys.* **113** 034902.

Table 1: Summary of the measurement results for the electron emissions induced by a pyroelectric crystal and extracted by an external acceleration voltage, when a diode was (or not) connected between the cathode and ground. A negative pulse was applied to the front electrode of the cathode, the nominal break down voltage for the spark gap was 1.5 kV. The distance between the anode and cathode was 10 mm. The extraction voltage, peak current, and total charges were all measured at the anode, which had a diameter of 12.5 mm. The cathode grid electrode was a 50 mesh TEM grid made of Copper.

	Extraction (V)	ΔT (K)	Peak Current (mA)	Total Charge (nC)	Pyro Charge (nC)	Total Charge / Pyro Charge
	0	20.4	-12.5	-3.9	-74.6	5%
	93	20.3	-18.6	-7.6	-74.2	10%
	227	19.2	-40.1	-28.7	-70.2	41%
	425	19.2	-55	-27	-70.2	38%
	678	18.8	-77.6	-37.9	-68.7	55%
	861	19.8	-82.4	-40	-72.4	55%
	1243	21.7	-95	-72.3	-79.3	91%
No Diode	1610	21.1	-99.4	-88.9	-77.1	115%
	0	18.3	-22.1	-11.1	-66.9	17%
	121	19.6	-32.2	-10.4	-71.6	15%
	254	19.8	-50.7	-25.9	-72.4	36%
	439	19.6	-73.3	-30.2	-71.6	42%
	656	19.1	-87.8	-55.8	-69.8	80%
	894	21.4	-100	-76.1	-78.2	97%
With Diode	1030	19.6	-143	-83.5	-71.6	117%

Table 2: Summary of the results for the electron emissions induced and extracted by pyroelectric crystals when the charge storage capacitor C_{acc} was 10 pF and with a diode being connected between the cathode and ground. ΔT_{acc} is the temperature change of the extracting pyroelectric crystal, ΔT_{chg} is the temperature change of the pulse generating crystal, V_{acc} is the anode extracting voltage at the beginning of electron emission, Q_{acc} is the total charges generated by the anode crystal, Q_{pulse} is the total charges generated by the pulse crystal, Q_{col}/Q_{acc} is the ratio between the collected charges at the anode and the total anode charges, Q_{col}/Q_{pulse} is the ratio between the collected charges and the total pulse charges.

ΔT_{acc} (K)	ΔT_{pulse} (K)	V_{acc} (V)	Q_{col} (nC)	Q_{acc} (nC)	Q_{col} / Q_{acc}	Q_{pulse} (nC)	Q_{col} / Q_{pulse}
0	20.8	0	-3	0	-	-75.9	4.0%
2.6	22.3	774	-5.8	9.5	-61.1%	-81.4	7.1%
4.5	20.2	1300	-10.3	16.4	-62.7%	-73.7	14.0%
6.7	18.4	1909	-19.2	24.5	-78.5%	-67.2	28.6%
8.7	20.2	2462	-22.1	31.8	-69.6%	-73.7	30.0%
12.2	22.3	3430	-29.9	44.5	-67.1%	-81.4	36.7%
13.9	22.4	3901	-32.4	50.7	-63.9%	-81.8	39.6%
18.1	21.3	5063	-41.3	66.1	-62.5%	-77.7	53.1%

Figure Captions

Figure 1 (a) Schematic of the pulse generation, ferroelectric cathode and anode subsections of the pyroelectric crystal based electron beam generator; a: Peltier temperature controller; b: pyroelectric crystal; c: external charging capacitor; d: rear electrode and the ferroelectric material; e: patterned front electrode; f: anode; g: miniature spark gap switch. The equivalent circuits including the measurement components for the pyroelectric crystal induced and extracted electron beam generator (b); pyroelectric crystal induced and external voltage extracted electron beam generator (c).

Figure 2 Profiles against time of the cathode voltage and collected current and total charges at the anode for different extracting voltages: (a) 227 V; (b) 1610 V.

Figure 3 The relationship between the final voltage on the cathode and the extracting voltage on the anode.

Figure 4 Profiles against time of the cathode voltage V_{cat}, voltage on the charging capacitor V_{chg}, and the emission current as collected at the anode I_{anode} under different extracting voltages, (a) 0V; (b) 200 V and (c) 600 V.

Figure 5 The relationship between the residual voltage on the charging capacitor C_{chg} and the extracting voltage on the anode.

Figure 6 Schematic of the emission system including a cathode, an anode, and a shunt diode connected between the front electrode of the cathode and the ground. The diode enables the discharge of the positive charges on the cathode.

Figure 7 The collected emission charges as a function of extracting voltage with or without a diode being connected between the cathode and ground when the anode charge storage capacitor C_{acc} being 50 pF. The inducing voltage was generated by a pyroelectric crystal and the extracting voltage was provided by an external DC voltage source. Figure 8 The collected emission charges as functions of extracting voltage with or without a diode being

connected between the cathode and ground for different anode charge storage capacitance: (a) 50 pF; (b) 10 pF. Both the inducing and extracting voltages were generated by pyroelectric crystals.

Figure 9 Comparison of the total collected emission charges as functions of the extracting voltage when the anode were a pyroelectric crystal connected with a 10 pF, 50 pF charge storage capacitor, and an external high voltage source with capacitance of 13 nF.

Figure 10 Time profiles of (a) voltage at the cathode, and (b) charges collected at the anode for different acceleration voltages, with the charging storage capacitor C_{acc} being 50 pF and a diode was connected between the cathode and ground. Both the inducing and extracting voltages were generated by pyroelectric crystals.

Figure 11 Time profiles of (a) voltage at the cathode, and (b) charges collected at the anode for different acceleration voltages, with the charging storage capacitor C_{acc} being 10 pF and no diode was connected between the cathode and ground. Both the inducing and extracting voltages were generated by pyroelectric crystals.

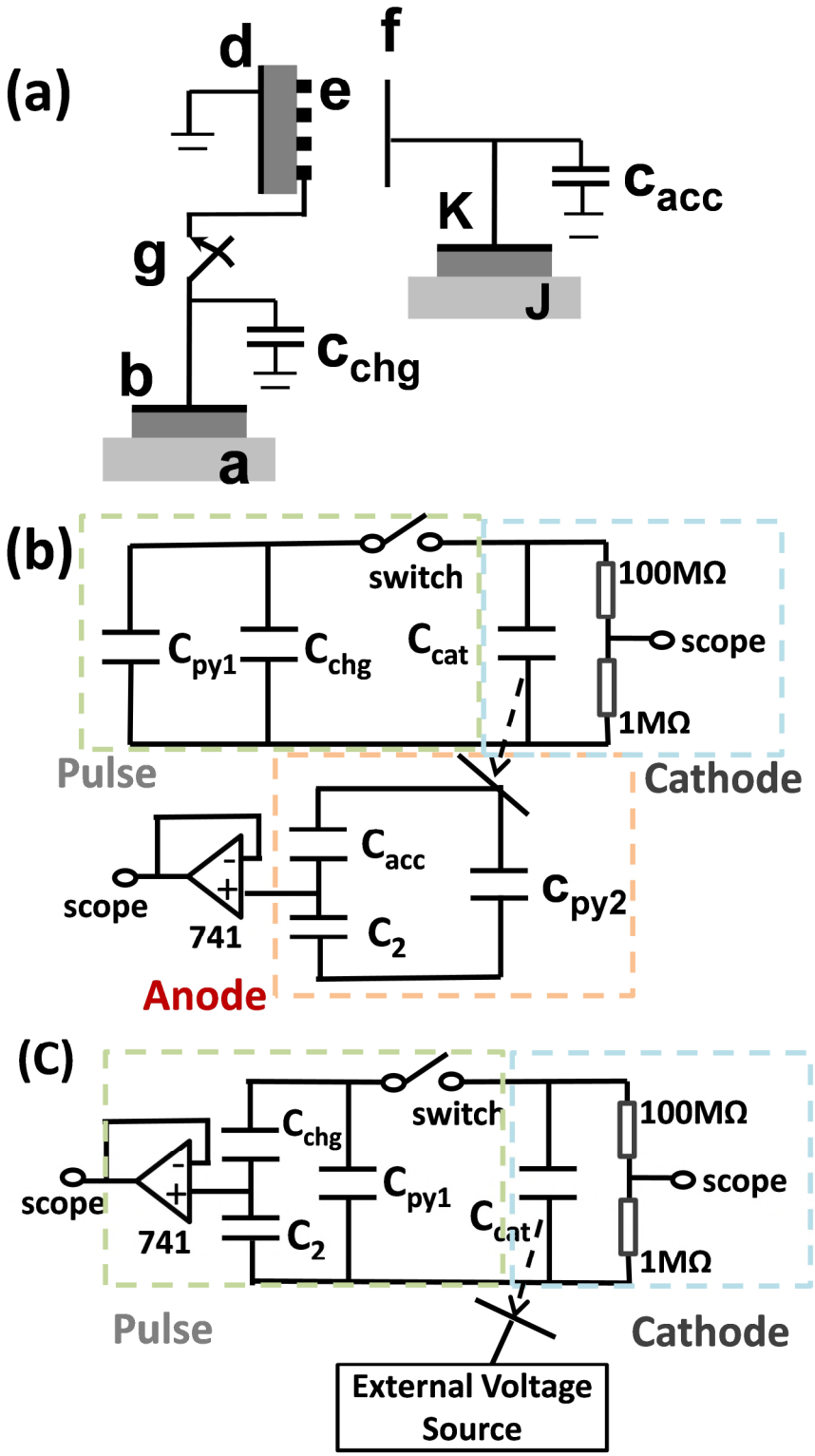
(a)
d
e
f
g
b
a
K
J
C_{acc}
C_{chg}
(b)
switch
100MΩ
scope
1MΩ
C_{py1}
C_{chg}
C_{cat}
Pulse
Cathode
scope
741
C_{acc}
C_{py2}
C_2
Anode
(C)
switch
100MΩ
scope
1MΩ
C_{chg}
C_{py1}
C_{cat}
scope
741
C_2
Pulse
Cathode
External Voltage Source

Figure 1

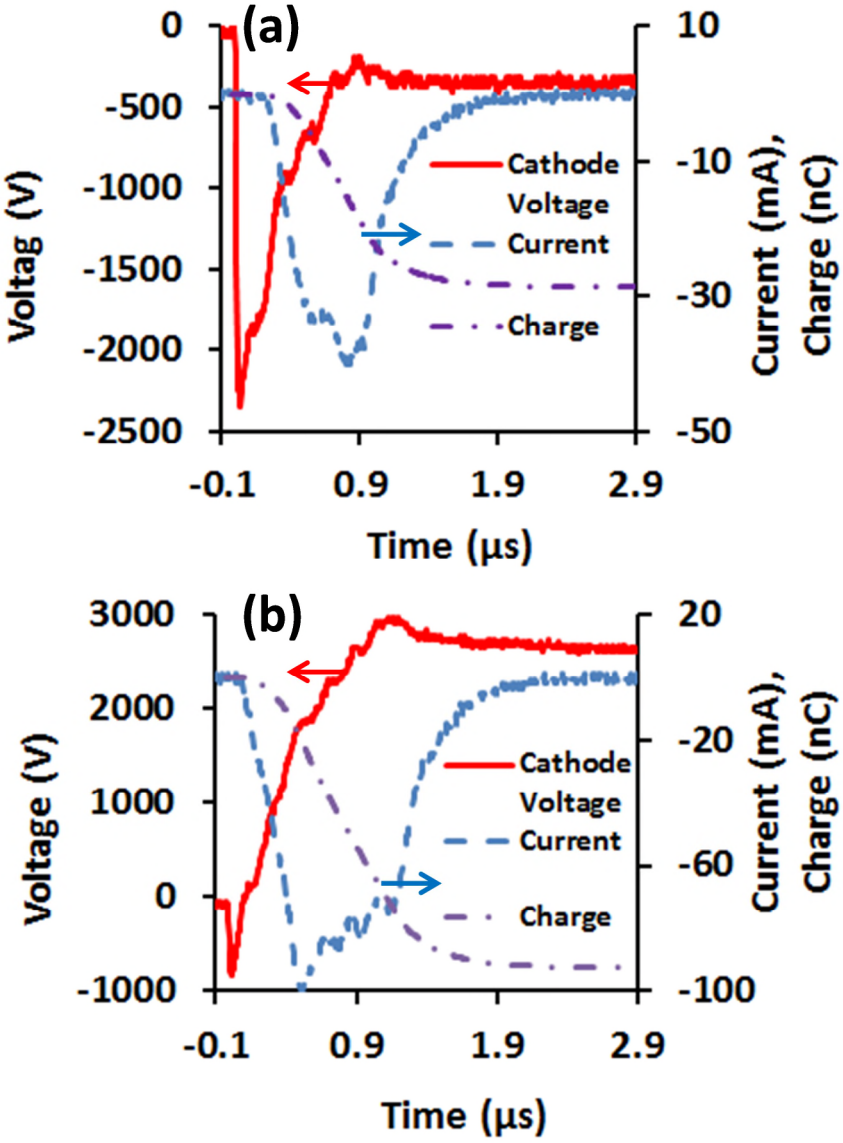
(a)
0
-500
-1000
-1500
-2000
-2500
Voltag (V)
10
-10
-30
-50
Current (mA), Charge (nC)
Cathode Voltage
Current
Charge
-0.1
0.9
1.9
2.9
Time (µs)
(b)
3000
2000
1000
0
-1000
Voltage (V)
20
-20
-60
-100
Current (mA), Charge (nC)
Cathode Voltage
Current
Charge
-0.1
0.9
1.9
2.9
Time (µs)

Figure 2

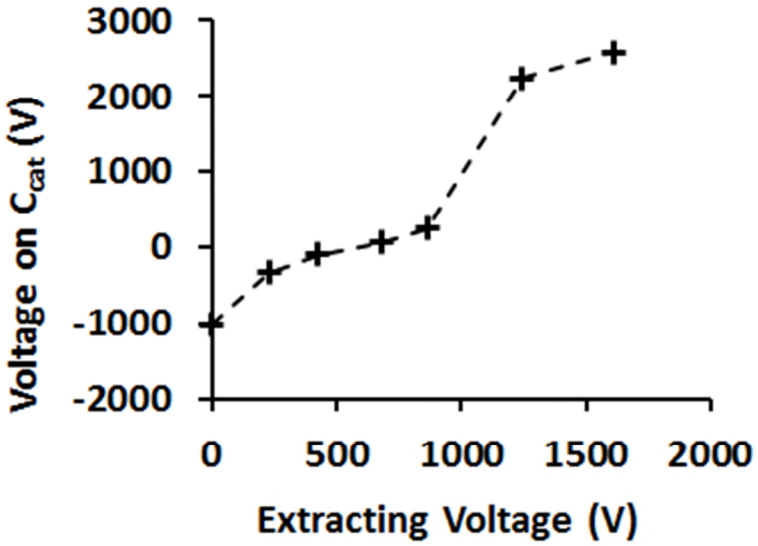
3000
2000
1000
0
-1000
-2000
Voltage on C_{cat} (V)
0
500
1000
1500
2000
Extracting Voltage (V)

Figure 3

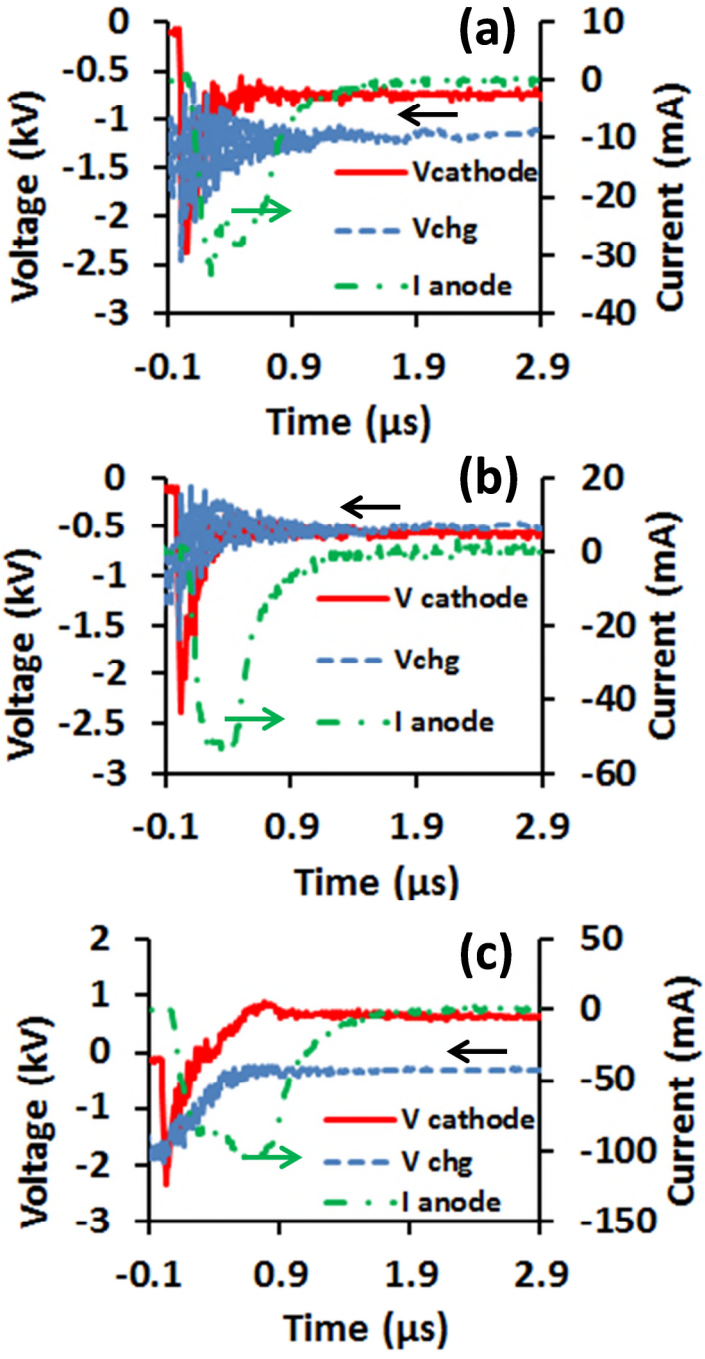
(a)
Voltage (kV)
Current (mA)
Time (µs)
Vcathode
Vchg
I anode
(b)
V cathode
Vchg
I anode
(c)
V cathode
V chg
I anode

Figure 4

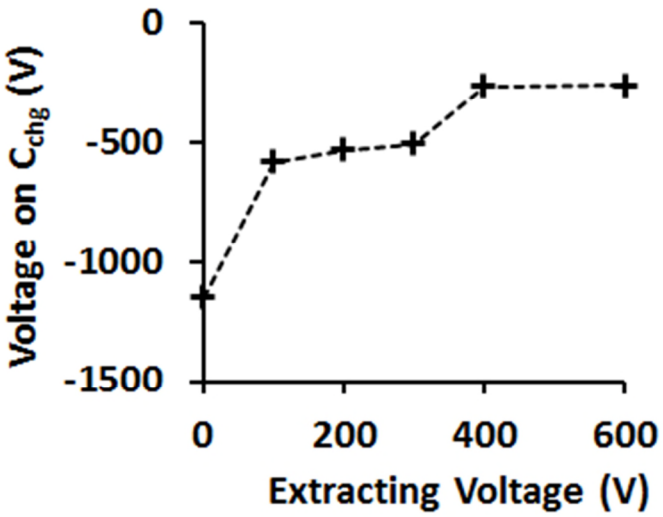
0
-500
-1000
-1500
Voltage on C_{chg} (V)
0
200
400
600
Extracting Voltage (V)

Figure 5

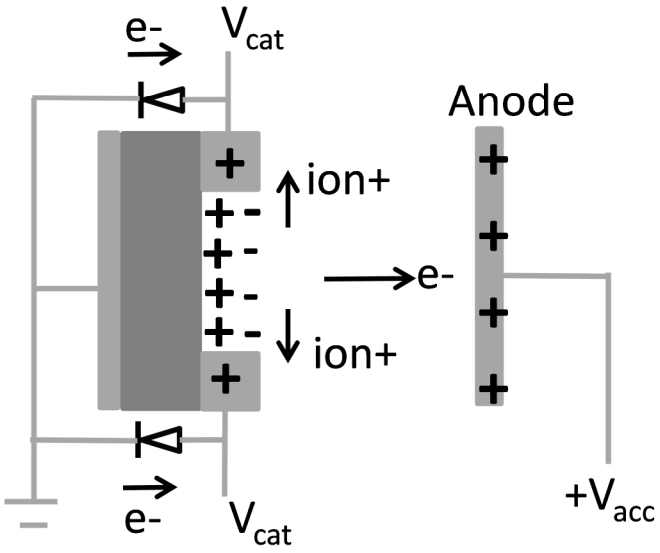

Figure 6

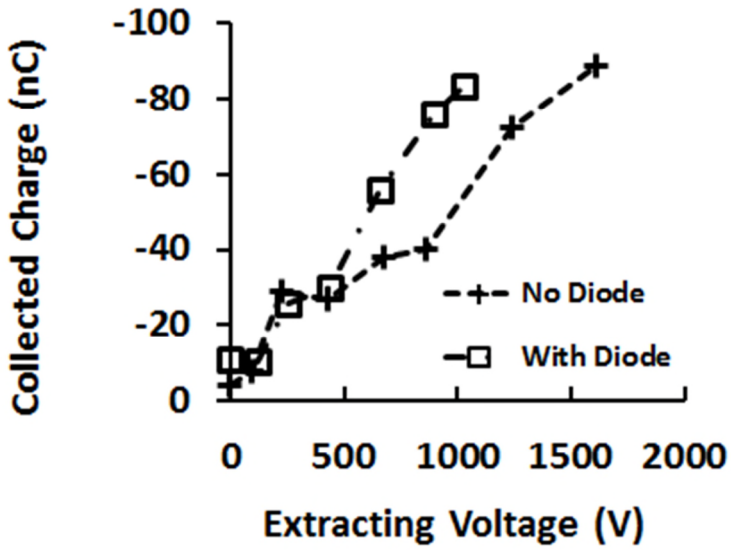
-100
-80
-60
-40
-20
0
Collected Charge (nC)
No Diode
With Diode
0
500
1000
1500
2000
Extracting Voltage (V)

Figure 7

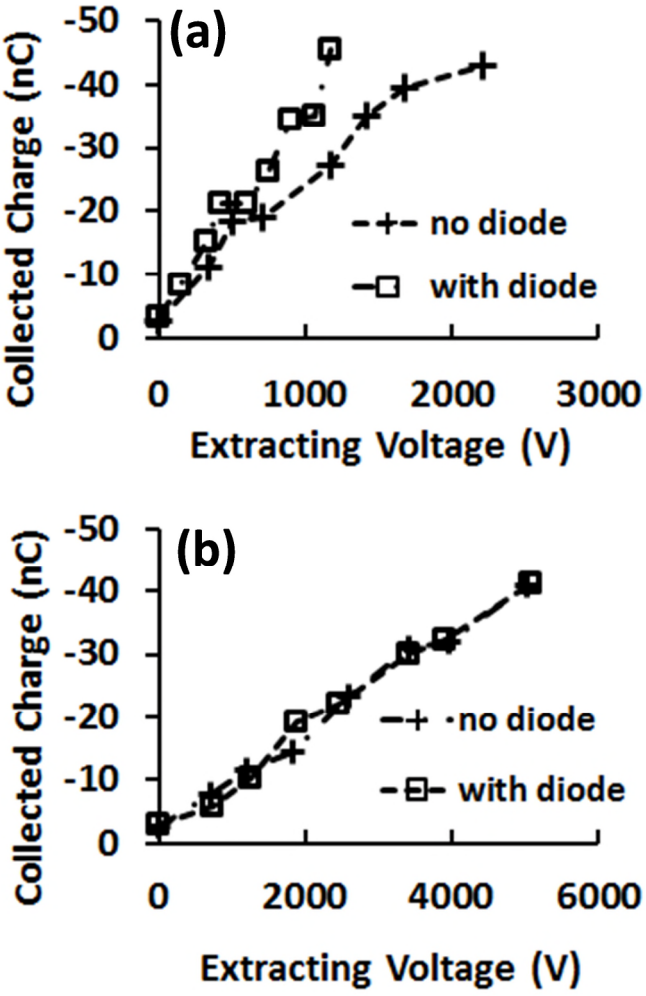
(a)
Collected Charge (nC)
-50
-40
-30
-20
-10
0
no diode
with diode
0
1000
2000
3000
Extracting Voltage (V)
(b)
Collected Charge (nC)
-50
-40
-30
-20
-10
0
no diode
with diode
0
2000
4000
6000
Extracting Voltage (V)

Figure 8

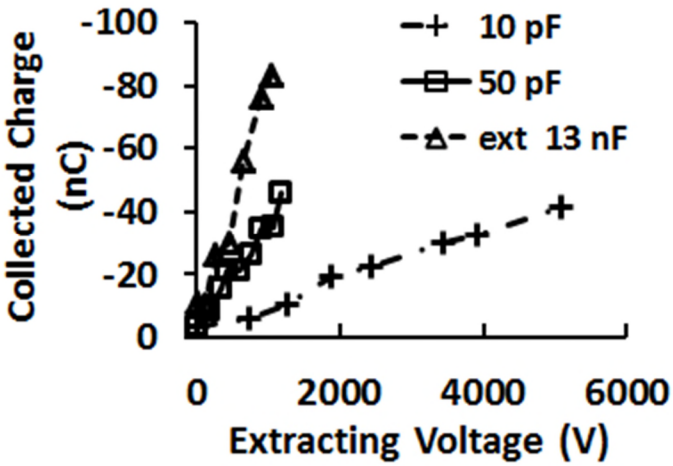
Collected Charge (nC)
-100
-80
-60
-40
-20
0
0
2000
4000
6000
Extracting Voltage (V)
10 pF
50 pF
ext 13 nF

Figure 9

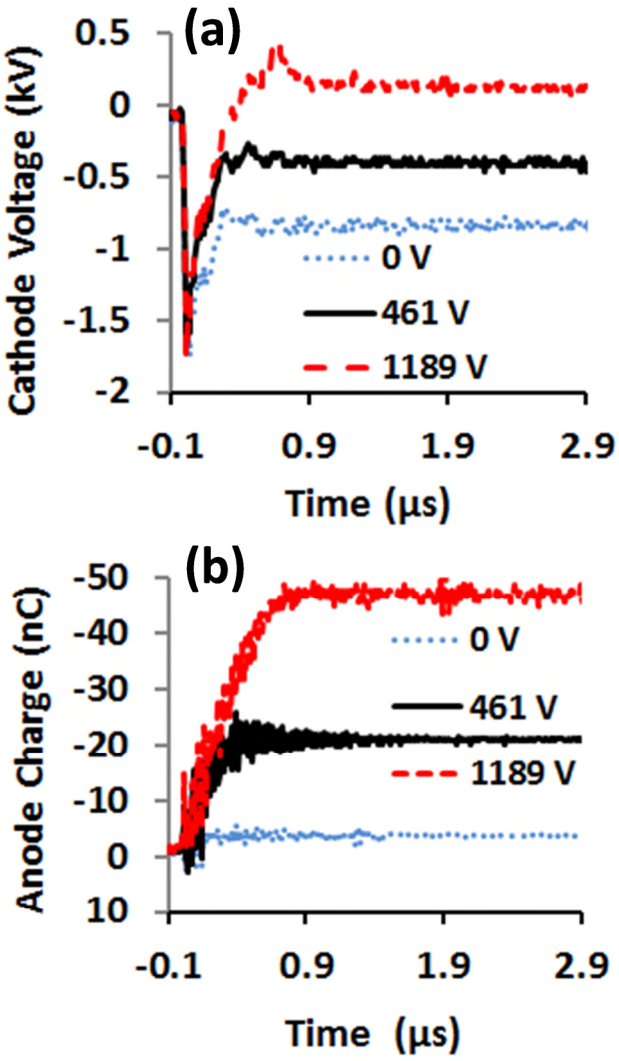
(a)
Cathode Voltage (kV)
0.5
0
-0.5
-1
-1.5
-2
0 V
461 V
1189 V
-0.1
0.9
1.9
2.9
Time (µs)
(b)
Anode Charge (nC)
-50
-40
-30
-20
-10
0
10
0 V
461 V
1189 V
-0.1
0.9
1.9
2.9
Time (µs)

Figure 10

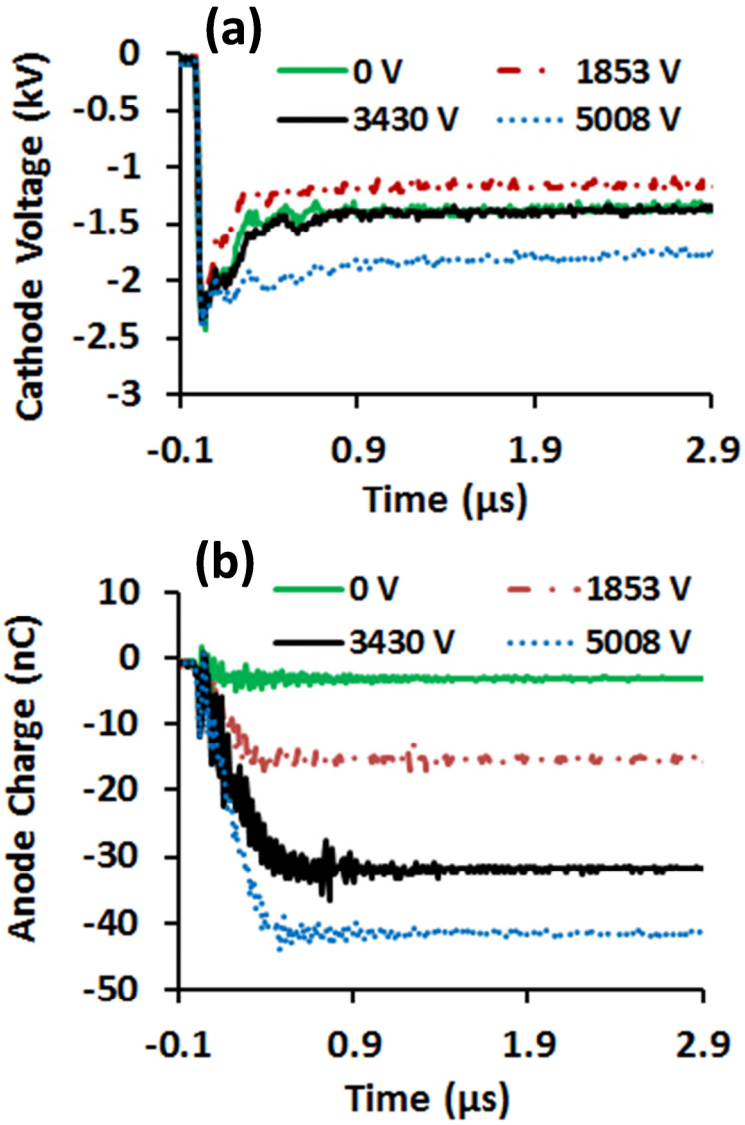
(a)
0 V
1853 V
3430 V
5008 V
Cathode Voltage (kV)
0
-0.5
-1
-1.5
-2
-2.5
-3
-0.1
0.9
1.9
2.9
Time (µs)
(b)
0 V
1853 V
3430 V
5008 V
Anode Charge (nC)
10
0
-10
-20
-30
-40
-50
-0.1
0.9
1.9
2.9
Time (µs)

Figure 11